Published in final edited form as:

Environ Toxicol. 2022 February ; 37(2): 237–244. doi:10.1002/tox.23393.

ROS generation is involved in titanium dioxide nanoparticleinduced AP-1 activation through p38 MAPK and ERK pathways in JB6 cells

Lu Kong[1,2], **Tabatha Barber**[2], **Joni Aldinger**[2], **Linda Bowman**[2], **Stephen Leonard**[3], **Jinshun Zhao**[2], **Min Ding**[2]

[1]Key Laboratory of Environmental Medicine and Engineering, Ministry of Education; School of Public Health, Southeast University, Nanjing, China

[2]Toxicology and Molecular Biology Branch, Health Effects Laboratory Division, National Institute for Occupational Safety and Health, Morgantown, West Virginia, USA

[3]Pathology and Physiology Research Branch, Health Effects Laboratory Division, National Institute for Occupational Safety and Health, Morgantown, West Virginia, USA

Abstract

Titanium dioxide (TiO_2) is generally regarded as a nontoxic and nongenotoxic white mineral, which is mainly applied in the manufacture of paper, paint, plastic, sunscreen lotion and other products. Recently, TiO_2 nanoparticles (TiO_2 NPs) have been demonstrated to cause chronic inflammation and lung tumor formation in rats, which may be associated with the particle size of TiO_2. Considering the important role of activator protein-1 (AP-1) in regulating multiple genes involved in the cell proliferation and inflammation and the induction of neoplastic transformation, we aimed to evaluate the potency of TiO_2 NPs (≤ 20 nm) on the activation of AP-1 signaling pathway and the generation of reactive oxygen species (ROS) in a mouse epidermal cell line, JB6 cells. MTT, electron spin resonance (ESR), AP-1 luciferase activity assay in vitro and in vivo, and Western blotting assay were used to clarify this problem. Our results indicated that TiO_2 NPs dose-dependently caused the hydroxyl radical (·OH) generation and sequentially increased the AP-1 activity in JB6 cells. Using AP-1-luciferase reporter transgenic mice models, an obvious increased AP-1 activity was detected in dermal tissue after exposure to TiO_2 NPs for 24 h. Interestingly, TiO_2 NPs increased the AP-1 activity via stimulating the expression of mitogen-activated protein kinases (MAPKs) family members, including extracellular signal-regulated protein kinases (ERKs), p38 kinase, and C-Jun N-terminal kinases (JNKs). Of note, the AP-1 activation induced by TiO_2 NPs could be blocked by specific inhibitors (SB203580, PD98059, and SP 600125, respectively) that inhibit ERKs and p38 kinase but not JNKs. These findings indicate that ROS generation is involved in TiO_2 NPs-induced AP-1 activation mediated by MAPKs signal pathway.

Correspondence: Lu Kong, Key Laboratory of Environmental Medicine and Engineering, Ministry of Education, School of Public Health, Southeast University, Nanjing 210009, China., konglu_yaoyu@126.com.

CONFLICT OF INTEREST

The authors declare no conflicts of interest.

Keywords

activator protein-1 (AP-1); JB6 cells; mitogen-activated protein kinases (MAPKs); reactive oxygen species (ROS); titanium dioxide nanoparticles (TiO_2 NPs)

1 | INTRODUCTION

Nanomaterials have attracted people's attention in electronics, reinforcement rods, micro-manufacturing, cosmetics, and nanomedicine.[1–3] Especially, the development of nanomaterials has grown exponentially in the past 10 years. As expected, the number of people who produce or use nanomaterials increases accordingly. However, limited information is available regarding the potential mechanism of the carcinogenesis of nanoparticles. It has been demonstrated that the physical and chemical properties of nanoparticles possess a strongly influence on their biological actions,[4–6] and titanium dioxide nanoparticles (TiO_2 NPs) were nearly spherical anatase crystals modified with hydroxyl group on the surface.[7] TiO_2 NPs are naturally occurring mineral substances and widely applied in cosmetics, paint, and pharmaceuticals. Up to now, it is generally considered to be nontoxic, nongenotoxic, and widely used as an inert control in toxicologic studies.[8–11] However, experimental studies in rats and epidemiological population surveys verified that the exposure to TiO_2 NPs could lead to the development of pulmonary inflammation, tissue damage and fibrosis, and even lung tumors.[12–18] It was reported earlier that rats developed chronic inflammation and tumors after tracheal instillation of TiO_2 fine particles (TiO_2 FPs) (0.25 μm) and TiO_2 NPs (21 nm),[19–24] and pulmonary inflammation and hyperplasia were observed at all exposure levels. Compared with TiO_2 FPs, TiO_2 NPs could impair macrophage function with persistently high-inflammatory reactions, thus increasing pulmonary retention.[13] Furthermore, the levels of specific mRNA related to tumor necrosis factor, interleukin 1 (IL-1), IL-6, and IL-8 were raised after exposure of human alveolar macrophages to TiO_2 NPs.[25] Simultaneously, it was confirmed that reactive oxygen species (ROS) was generated in rat and human alveolar macrophages during the process of degrading TiO_2 NPs by luminol-dependent chemiluminescence assay. To date, there are limited data on dermal effects of TiO_2 NPs among humans. With the advent of nanotechnology, the skin, whether consciously or unconsciously, can be exposed to solid nanoscale particles. Intentionally added nanomaterials are being developed in the application of lotions or creams containing nanoscale TiO_2 or ZnO as sunscreen components, whereas unintentional dermal exposure that occurs when paints or coatings containing nanoscale substances are used to achieve waterproof or anti-fouling properties, or when skin directivity contact with anthropomorphic substances produced during the manufacturing or burning of nanomaterials is involved.[26] However, there were limited data on dermal effects after personal exposure to nanoscale TiO_2 in our living surroundings.

Many stimuli, especially ROS, are able to stimulate activator protein-1 (AP-1) by binding to the promoter regions of multiple genes that play a vital role in modulating inflammation, cell proliferation, apoptosis, and carcinogenesis.[27,28] The increase of AP-1 activity is related to malignant transformation and the action of tumor promoting agents, such as growth factors, ultraviolet radiation, and transforming oncogenes.[29,30] Blocking 12-O-

tetradecanoylphorbol-13-acetate (TPA)-induced AP-1 activation has been documented to suppress the neoplastic transformation.[31,32]Considering the pivotal role of AP-1 on the inflammation and carcinogenesis, we aimed to investigate the effects of TiO_2 NPs on the skin in vitro and in vivo via activating AP-1 and its related signal mitogen-activated protein kinases (MAPKs). As we know, p38 kinase, extracellular signal-regulated protein kinases (ERKs), and C-Jun N-terminal kinases (JNKs) are the three major MAPKs, which are responsibility for c-Jun phosphorylation and AP-1 activation.[33–36] Dhar et al. demonstrated that JB6 mouse epidermal cells were valuable for monitoring early signaling events in oxidative stress related to carcinogenesis.[37] To test the mechanisms involved, JB6 cells were investigated to confirm the TiO_2 NPs-induced hydroxyl radical (·OH) generation and activation of MAPKs pathways underlying the AP-1 activation. Herein, we demonstrate that TiO_2 NPs induce AP-1 activation, and such activation may occur through the ERK1/2 and p38 MAPKs kinase signal transduction pathways in JB6 cells.

2 | MATERIALS AND METHODS

2.1 | Reagents

5,5-dimethyl-1-pyrroline-*N*-oxide (DMPO) and catalase were purchased from Sigma Chemical CO. (St. Louis, MO) and Boehringer Mannheim (Indianapolis, IN), respectively. The methods including charcoal decolorization and vacuum distillation were used to purify the spin trap DMPO, therefore, the purified DMPO solution should not contain any detectable impurities by electron spin resonance (ESR) spectroscopy. Chelex 100 chelating resin was obtained from Bio-Rad Laboratories (Richmond, CA), which was used to remove contaminants containing transition metal ions in phosphate buffer (pH 7.4). Eagle's minimum essential medium (MEM) and luciferase assay substrate were, respectively, obtained from Whittaker Biosciences (Walkersville, MD) and Promega (Madison, WI). Fetal bovine serum (FBS), gentamicin, and L-glutamine were from Life Technologies, Inc. (Gaithersburg, MD). Phospho Plus MAPK Antibody Kits and 3-(4, 5-dimethylthiazol-2-yl)-2,5,-diphenyl tetrazolium bromide (MTT) Cell Proliferation Assay were purchased from New England Bio Labs (Beverley, MA) and Sigma-Aldrich (Saint Louis, MO, USA), respectively. TiO_2 NPs with a diameter of less than 20 nm and a specific surface area of more than 400 m^2/g were obtained from Nano Active (Manhattan, KS), and TiO_2 FPs with a diameter of less than 5 μm were purchased from Sigma-Aldrich (St. Louis, MO).[38]

2.2 | Cell culture

First, JB6 cells were stably transfected with an AP-1 luciferase reporter plasmid,[39] and then cultured in Eagle's MEM supplied with 5% FBS, 2 mM L-glutamine, and 50 μg gentamicin/ml under standard culture conditions.

2.3 | Cell viability assay

MTT Cell Proliferation assay was performed in this study to ascertain cell viability after exposure to 25–200 $\mu g/cm^2$ TiO_2 NPs or TiO_2 FPs. JB6 cells (1×10^4 cells/well) were plated in a 96-well plate and then cultured with or without particles. Following incubation for 48 h, 10 μl MTT solution were added to each well and further incubated for another 4 h. Then, 100 μl solubilization solution were added and incubated overnight at 37°C. Thereafter,

the optical density (OD) was measured on an ELISA plate reader at a wavelength of 590 nm. The result is calibrated with the OD measured in the absence of cells.

2.4 | ROS measurements

ESR was utilized in this study to demonstrate potential induction of radical generation after exposure to TiO_2 NPs or TiO_2 FPs for various time. Briefly, reactants were carried out in a final volume of 450 μl in test tubes, and then the reaction mixture was then placed in a flat cell for the measurement of ESR spectra using a Varian E9 ESR spectrometer. Meanwhile, reference standards were done by measuring the hyperfine couplings (to 0.1 G) directly from magnetic field separation in comparison with K_3CrO_8 and DPPH. All experiments were carried out under ambient air and at room temperature except those specifically indicated. Experimental data acquisitions and analyses were performed by EPRDAP 2.0 program, and the final concentration was shown in the legend.

2.5 | In vitro AP-1 luciferase activity assay

The AP-1 transcription factor is usually expressed at low basal level, however it can be remarkably activated by many different stimuli,[42] therefore the effect of TiO_2 NPs on AP-1 activity was studied in our current study. Briefly, JB6 AP-1 cells were digested with trypsin, incubated with Eagle's MEM(5% FBS) in a 24-well plate at 5×10^4 cells/well and placed in a 5% CO_2 humidified atmosphere at 37°C. After 12 h, the cells were incubated with Eagle's MEM with 0.1% FBS for another 12–24 h to minimize the basal activity of AP-1. Thereafter, the cells were then exposed to the ultrasonically dispersed TiO_2 NPs in the same medium for 24 h to monitor the inhibitory effect of AP-1 activity. According to the detection steps of the luciferase assay kit, 200 μl 1 × lysis buffer were added to extract the cells, then the luciferase activity was detected on a 3010 monolight luminometer,[39] and the relative AP-1 activity was calculated as normalized to untreated cells.

2.6 | In vivo AP-1 luciferase activity assay

C57BL/6 mice and the founder stocks for these mice were a gift given by the University of Minnesota. Following the surface area of TiO_2 NPs and TiO_2 FPs characterized previously by our laboratory,[38] AP-1-luciferase reporter C57BL/6 crossed with DBA2 transgenic mice were carried out to explore the effect of TiO_2 NPs on AP-1 activity in vivo. In brief, mice were fed and kept at the West Virginia University Animal Facility, and all studies were in accordance with experimental protocols approved by the West Virginia University Animal Care and Use Committee. These mice were monitored in absence of specific pathogens, housed in plastic filter-top cages on corncob bedding, and given autoclaved tap water and Prolab 3500 feed ad libitum. 24–28 male and female mice were used in each group. After shaving the hair on the back skin of the mice, TiO_2 NPs (1 mg TiO_2 NPs dissolved in 0.3 ml acetone) were applied for topical treatment, meanwhile acetone alone was used in the control group. Of note, liquid acetone on the skin will have a mild irritation, resulting in a small risk of absorption through the intact skin.[40] After exposure for 24 h, the luciferase activity was measured in the samples of dorsal skin punch biopsy as previously described.[41] In short, the skin tissues were sampled with a 1.5 mm biopsy punch (Acuderm Inc. Ft. Lauderdale, FL) after the exposure of mice to TiO_2 NPs. Thereafter, the tissue was dissolved

in 4°C lysis buffer for 12 h, and then the supernatant was collected to measure the luciferase activity.

2.7 | Protein kinase phosphorylation assay

Western blotting assay was carried out to determine the phosphorylation levels of ERKs, JNKs, and p38 kinase in according to the protocol of New England Biolabs (Beverly, MA). Briefly, the cultured JB6 cells in different groups were collected, homogenized, and separated by 10% SDS-PAGE. After electrophoresis, samples were transferred to PVDF membranes and incubated with diluted phospho-specific antibodies against phosphorylated sites of ERKs, JNKs, and p38 kinase (1:1000). Meanwhile, non-phospho-specific antibodies against ERKs, JNKs, and p38 kinase proteins provided in each assay kit were used to normalize the phosphorylation assay by using the same-transferred membrane blot.

2.8 | Statistical analysis

Data were presented as means ± standard errors (SE), and the values were analyzed using one-way ANOVA or Student's *t* test. Significance was set at $p \leq .05$.

3 | RESULTS

3.1 | Effect of TiO_2 NPs on cell viability

After treatment with TiO_2 NPs for 48 h, the results of MTT assay confirmed that TiO_2 NPs at doses of 25–100 μg/cm^2 had no obviously inhibitory effect on cell viability, while high dose of TiO_2 NPs (200 μg/cm^2) significantly inhibited cell viability compared with control group ($p < .05$) (Figure 1).

3.2 | Effect of TiO_2 NPs on stimulation of ROS generation in the cultured JB6 cells

ROS generation was detected in the process of cellular reaction and in the presence of TiO_2 NPs or TiO_2 FPs by ESR spin trapping technology. After exposure to DMPO with or without TiO_2 NPs (or TiO_2 FPs), no detectable radical signal was observed (Figure 2A-a, b, c, and d). Of note, after exposure of JB6 cells to TiO_2 NPs with DMPO, it was detected that a spin adduct signal (Figure 2A-f) consisting of a 1:2:2:1 quartet with hyperfine splitting of parameters ($a_N = a_H = 14.8$ G), where a_N and a_H stand for nitroxyl nitrogen and *a*-hydrogen, respectively. On the basis of this splitting and the line shape of 1:2:2:1, the formed spectrum of DMPO-OH adducts could represent the formation of the ·OH radical. As shown in Figure 2, JB6 cells incubated with TiO_2 FPs and DMPO (Figure 2A-e) generated less ·OH radical than those with TiO_2 NPs and DMPO, and the average ESR peak (Figure 2B) indicated that TiO_2 NPs were more potential to stimulate ROS generation than TiO_2 FPs. Notably, after exposure of JB6 cells (1×10^6) to 200 mM DMPO with 1 mg/ml TiO_2 FPs (or TiO_2NPs) for 5, 10, and 15 min, the time course study suggested that ·OH radical was generated immediately once the JB6 cells were mixed with TiO_2 NPs, and it time-dependently increased for up to 15 min (Figure 3A,B).

As shown in Figure 4, there were no obvious signal in DMPO with or without JB6 cells groups (Figure 4A-a and b). Interestingly, exposure of JB6 cells to TiO_2 NPs remarkably increased the signal intensity (Figure 4A-c,B), which was reversed by additional catalase

(Figure 4A-c,B), indicating the importance role of hydrogen peroxide. Simultaneously, additional deferoxamine could chelate the metal ions such as Fe (II) and make them less reactive toward hydrogen peroxide (Figure 4A-e,B), consequently decreasing the signal intensity. All these results indicate that a metal-mediated Fenton or Fenton-like reaction plays a role in ·OH generation in the JB6 cells treated with TiO_2 NPs. Furthermore, additional hydrogen peroxide increased the signal intensity in JB6 cells compared with those without (Figure 4A-c, f, and B).

3.3 | Effect of TiO_2 NPs on AP-1 luciferase activity in vitro and in vivo experiments

In a certain range of concentration, TiO_2 NPs dose-dependently induced AP-1 activation in JB6 cells and the AP-1 activation reached its maximum level at the dose of 12.5 μg/cm^2. In addition, TiO_2 NPs possessed greater potential to increase AP-1 activation than TiO_2 FPs at low concentration of 0–12.5 μg/cm^2. After that, with increasing concentrations of TiO_2 NPs, the AP-1 activation in JB6 cells decreased, probably due to the TiO_2 NPs-induced cell cytotoxicity and/or growth inhibition (Figure 5). Notably, AP-1 activity was close to zero, whereas the cell vitality was still at a high level when the concentration of TiO_2 NPs reached to 100 μg/cm^2 (Figure 5), thus100 μg/cm^2 TiO_2 NPs were selected to prove the inhibitory effect of several kinases' inhibitors on AP-1 activity. Additionally, the AP-1 activity increased slowly within a certain range. Furthermore, using AP-1-luciferase reporter C57BL/6 crossed with DBA2 transgenic mice models, an obvious increased AP-1 activity was detected in dermal tissue of mice after exposed to TiO_2 NPs for 24 h. However, no obviously changes of AP-1 activity were in dermal tissues from the TiO_2 FPs group compared with control group (Figure 6), suggesting that TiO_2 NPs possess greater potential to induce AP-1 activation, owning to the nanolevel particle size.

3.4 | Effects of TiO_2 NPs on the expression of MAPKs in JB6 Cells

As shown in Figure 7A, with the increasing concentrations of TiO_2 NPs at a range of 0–200 μg/cm^2, the phosphorylation levels of p38 kinase, ERKs and JNKs were upregulated in the JB6 cells in a dose-dependent manner (Figure 7A). Similarly, upregulation of the expression of MAPKs was also detected in TiO_2 FPs group (Figure 7B). In addition, TiO_2 NPs at the dose of 150 μg/cm^2 upregulated the phosphorylation levels of p38 kinases, ERKs, and JNKs in a time-dependent manner (Figure 7C). Of note, ERKs were the most rapidly responding kinases, following with JNKs and p38 kinase.

3.5 | Inhibitory effects of MAPKs inhibitors on TiO_2 NPs-induced AP-1 activation

After exposure to 100 μg/cm^2 TiO_2 NPs with or without MAPKs inhibitors, the results of AP-1 luciferase activity assay suggested that compared with untreated cells, TiO_2 NPs-induced AP-1 activation decreased significantly, and the increased AP-1 activation could be inhibited by either SB203580 (p38 inhibitor) or PD98059 (ERK inhibitor), but not SP600125 (JNK inhibitor) (Figure 8).

4 | DISCUSSION

Considering the complexities of epidemiologic studies and unresolved animal experimental tumor studies, the current studies focused on molecular mechanistic processes associated

with inflammation and carcinogenesis to provide some new insight on the potential of TiO_2 as a probable carcinogen.[42] In this respect, our researches on AP-1 activation through MAPK support the previous studies that TiO_2 NPs may be involved in the development of carcinogenic processes.[43] Notably, the in vitro and in vivo experiments confirmed that within a range of certain density, TiO_2 NPs possess greater potential to induce AP-1 activation thanTiO_2 FPs, which may be related to the nanolevel particle size.

AP-1, a dimeric complex, is composed of Jun and Fos protein families. Some AP-1-encoding genes, c-jun and c-fos, can be activated in response to various extracellular stimuli, and they maybe act as intermediate transcriptional regulators during the signal transduction, consequently leading to cell proliferation and malignant transformation. Following the activation of AP-1, downstream signal cascades including jun, fos, and other target genes can be triggered. These members of Jun and Fos protein families may involve in the cell signaling events via activating a specific receptor located on the cell surface with changes in gene expression that regulate cell responses, including cell proliferation and sequential phenotypic and functional changes. The vital content of this study is about that TiO_2 NPs stimulate the activation of AP-1 in both in vitro and in vivo models, which may be the key mechanism underlying the TiO_2 NPs-induced inflammation and/or carcinogenesis.

In recent years, the signal transduction pathways associated with the activation of transcription factors have been broadly researched. For example, it has been demonstrated that the activation of MAPK pathways (ERKs, JNKs, and p38) can be triggered by stress-related signals such as UV light or ROS. Some studies further confirmed that ERK, JNK, and p38 MAPK pathways can also be phosphorylated or activated by ROS, consequently leading to cell apoptosis.[44–46] As a major regulator of the transcriptional program, AP-1 is one of the downstream targets of MAPK members.[39] Accumulating evidence has documented that up-regulation of AP-1 play a vital role in the process of tumorigenesis.[47,48] In the present study, the possible mechanism underlying the role of ERKs, JNKs, and p38 MAPKs family in the induction of AP-1 activation has been investigated after exposure of JB6 cells to TiO_2 NPs. After pretreatment with the p38 inhibitor (SB203580) and ERK inhibitor (and PD98059) for 24 h, both of them inhibited AP-1 activity in JB6 cells induced by TiO_2 NPs, whereas pretreatment of cells with JNKs inhibitor (SP600125) had no obvious effect on the effect TiO_2 NPs-induced AP-1 activation. Thus, it can be inferred that TiO_2 NPs may phosphorylate ERKs and p38 kinase, but not JNKs. All these results indicate that TiO_2 NPs-induced AP-1 activation may be involved in the p38 kinase and ERKs pathways.

The results of this study provide novel insights to explore molecular mechanistic processes associated with inflammation and carcinogenesis of TiO_2 NPs and a great significance to develop safety evaluation criteria for TiO_2 NPs. However, the toxicity of TiO_2 NPs exposure should be further confirmed by animal experiments and epidemiological investigation. If possible, analyzing the toxic effect of different species induced by TiO_2 NPs will be helpful to formulate the criteria about safety assessment and rational use of TiO_2 NPs in the future.

5 | CONCLUSIONS

Using in vitro and in vivo models, it can be concluded that TiO_2 NPs stimulate the intracellular ROS generation and sequentially induce AP-1 activation through p38 MAPK and ERK pathways, which may be the key mechanisms underlying the TiO_2 NPs-induced inflammation and/or carcinogenesis. It is worth noting that elucidating the mechanisms involved in TiO_2 NPs-induced signaling pathway in parallel with the manipulation of target genes could provide insights for understanding the possible prevention of TiO_2 NPs-induced cytotoxicity and carcinogenesis.

Funding information

National Nature Science Foundation of China; the National Important Project on Scientific Research of China

DATA AVAILABILITY STATEMENT

Data sharing is not applicable to this article as no new data were created or analyzed in this study.

REFERENCES

1. Agostinelli E, Vianello F, Magliulo G, Thomas T, Thomas TJ. Nanoparticle strategies for cancer therapeutics: nucleic acids, polyamines, bovine serum amine oxidase and iron oxide nanoparticles (review). Int J Oncol. 2015;46(1):5–16. [PubMed: 25333509]
2. Li Z, Sun L, Lu Z, et al. Enhanced effect of photodynamic therapy in ovarian cancer using a nanoparticle drug delivery system. Int J Oncol. 2015;47(3):1070–1076. [PubMed: 26165140]
3. Zhao J, Bowman L, Magaye R, Leonard SS, Castranova V, Ding M. Apoptosis induced by tungsten carbide-cobalt nanoparticles in JB6 cells involves ROS generation through both extrinsic and intrinsic apoptosis pathways. Int J Oncol. 2013;42(4):1349–1359. [PubMed: 23417053]
4. Guichard Y, Schmit J, Darne C, et al. Cytotoxicity and genotoxicity of nanosized and microsized titanium dioxide and iron oxide particles in Syrian hamster embryo cells. Ann Occup Hyg. 2012;56(5):631. [PubMed: 22449629]
5. Jiang J, Oberdörster G, Elder A, Gelein R, Mercer P, Biswas P. Does nanoparticle activity depend upon size and crystal phase? Nanotoxicology. 2008;2(1):33–42. [PubMed: 20827377]
6. Pathakoti K, Manubolu M, Hwang HM. Effect of size and crystalline phase of TiO_2 nanoparticles on photocatalytic inactivation of *Escherichia coli*. J Nanosci Nanotechnol. 2019;19(12):8172–8179. [PubMed: 31196341]
7. Wang Y, Chen Z, Ba T, et al. Susceptibility of young and adult rats to the oral toxicity of titanium dioxide nanoparticles. Small (Weinheim an der Bergstrasse, Germany). 2013;9(9–10):1742–1752. [PubMed: 22945798]
8. Hedenborg M. Titanium dioxide induced chemiluminescence of human polymorphonuclear leukocytes. Int Arch Occup Environ Health. 1988;61(1–2):1–6. [PubMed: 3198275]
9. Ophus EM, Rode L, Gylseth B, Nicholson DG, Saeed K. Analysis of titanium pigments in human lung tissue. Scand J Work Environ Health. 1979;5(3):290–296. [PubMed: 20120578]
10. Warheit DB, Brown SC. What is the impact of surface modifications and particle size on commercial titanium dioxide particle samples?—a review of in vivo pulmonary and oral toxicity studies—revised 11-6-2018. Toxicol Lett. 2019;302:42–59. [PubMed: 30468858]
11. Hanot-Roy M, Tubeuf E, Guilbert A, et al. Oxidative stress pathways involved in cytotoxicity and genotoxicity of titanium dioxide (TiO2) nanoparticles on cells constitutive of alveolo-capillary barrier in vitro. Toxicol In Vitro: Int J Publ Assoc BIBRA. 2016;33:125–135.

12. Afaq F, Abidi P, Matin R, Rahman Q. Cytotoxicity, pro-oxidant effects and antioxidant depletion in rat lung alveolar macrophages exposed to ultrafine titanium dioxide. J Appl Toxicol: JAT. 1998;18(5):307–312. [PubMed: 9804429]
13. Baggs RB, Ferin J, Oberdörster G. Regression of pulmonary lesions produced by inhaled titanium dioxide in rats. Vet Pathol. 1997;34(6):592–597. [PubMed: 9396140]
14. Driscoll KE, Maurer JK. Cytokine and growth factor release by alveolar macrophages: potential biomarkers of pulmonary toxicity. Toxicol Pathol. 1991;19(4 Pt 1):398–405. [PubMed: 1667554]
15. Oberdörster G, Ferin J, Gelein R, Soderholm SC, Finkelstein J. Role of the alveolar macrophage in lung injury: studies with ultrafine particles. Environ Health Perspect. 1992;97:193. [PubMed: 1396458]
16. Wang Y, Cui H, Zhou J, et al. Cytotoxicity, DNA damage, and apoptosis induced by titanium dioxide nanoparticles in human non-small cell lung cancer A549 cells. Environ Sci Pollut Res Int. 2015;22(7):5519–5530. [PubMed: 25339530]
17. Yamadori I, Ohsumi S, Taguchi K. Titanium dioxide deposition and adenocarcinoma of the lung. Acta Pathol Jpn. 1986;36(5):783–790. [PubMed: 3739712]
18. Beck-Speier I, Karg E, Behrendt H, Stoeger T, Alessandrini F. Ultrafine particles affect the balance of endogenous pro- and anti-inflammatory lipid mediators in the lung: in-vitro and in-vivo studies. Part Fibre Toxicol. 2012;9:27. [PubMed: 22809365]
19. Bermudez E, Mangum JB, Wong BA, et al. Pulmonary responses of mice, rats, and hamsters to subchronic inhalation of ultrafine titanium dioxide particles. Toxicol Sci: Off J Soc Toxicol. 2004;77(2):347–357.
20. Churg A, Gilks B, Dai J. Induction of fibrogenic mediators by fine and ultrafine titanium dioxide in rat tracheal explants. Am J Physiol. 1999;277(5):L975–L982. [PubMed: 10564183]
21. Höhr D, Steinfartz Y, Schins RP, et al. The surface area rather than the surface coating determines the acute inflammatory response after instillation of fine and ultrafine TiO2 in the rat. Int J Hyg Environ Health. 2002;205(3):239–244. [PubMed: 12040922]
22. Lee KP, Trochimowicz HJ, Reinhardt CF. Pulmonary response of rats exposed to titanium dioxide (TiO2) by inhalation for two years. Toxicol Appl Pharmacol. 1985;79(2):179–192. [PubMed: 4002222]
23. Kolling A, Ernst H, Rittinghausen S, Heinrich U. Relationship of pulmonary toxicity and carcinogenicity of fine and ultrafine granular dusts in a rat bioassay. Inhal Toxicol. 2011;23(9):544–554. [PubMed: 21819261]
24. Nurkiewicz TR, Porter DW, Hubbs AF, et al. Pulmonary particulate matter and systemic microvascular dysfunction. Res Rep Health Eff Inst. 2011;164:3.
25. Drumm K, Buhl R, Kienast K. Additional NO2 exposure induces a decrease in cytokine specific mRNA expression and cytokine release of particle and fibre exposed human alveolar macrophages. Eur J Med Res. 1999;4(2):59–66. [PubMed: 10066641]
26. Oberdörster G, Oberdörster E, Oberdörster J. Nanotoxicology: an emerging discipline evolving from studies of ultrafine particles. Environ Health Perspect. 2005;113(7):823–839. [PubMed: 16002369]
27. Bernstein LR, Colburn NH. AP1/Jun function is differentially induced in promotion-sensitive and resistant JB6 cells. Science (New York, NY). 1989;244(4904):566–569.
28. Li JJ, Dong Z, Dawson MI, Colburn NH. Inhibition of tumor promoter-induced transformation by retinoids that transrepress AP-1 without transactivating retinoic acid response element. Cancer Res. 1996; 56(3):483–489. [PubMed: 8564958]
29. Adler V, Pincus MR, Polotskaya A, Montano X, Friedman FK, Ronai Z. Activation of c-Jun-NH2-kinase by UV irradiation is dependent on p21ras. J Biol Chem. 1996;271(38):23304–23309. [PubMed: 8798530]
30. Lamb RF, Hennigan RF, Turnbull K, et al. AP-1-mediated invasion requires increased expression of the hyaluronan receptor CD44. Mol Cell Biol. 1997;17(2):963–976. [PubMed: 9001250]
31. Li JJ, Westergaard C, Ghosh P, Colburn NH. Inhibitors of both nuclear factor-kappaB and activator protein-1 activation block the neoplastic transformation response. Cancer Res. 1997;57(16):3569–3576. [PubMed: 9270030]

32. Lin S, Li JJ, Fujii M, Hou DX. Rhein inhibits TPA-induced activator protein-1 activation and cell transformation by blocking the JNK-dependent pathway. Int J Oncol. 2003;22(4):829–833. [PubMed: 12632075]
33. Bernstein LR, Ferris DK, Colburn NH, Sobel ME. A family of mitogen-activated protein kinase-related proteins interacts in vivo with activator protein-1 transcription factor. J Biol Chem. 1994;269(13):9401–9404. [PubMed: 8144522]
34. Cowley S, Paterson H, Kemp P, Marshall CJ. Activation of MAP kinase kinase is necessary and sufficient for PC12 differentiation and for transformation of NIH 3T3 cells. Cell. 1994;77(6):841–852. [PubMed: 7911739]
35. Dérijard B, Hibi M, Wu IH, et al. JNK1: a protein kinase stimulated by UV light and Ha-Ras that binds and phosphorylates the c-Jun activation domain. Cell. 1994;76(6):1025–1037. [PubMed: 8137421]
36. Sturgill TW, Ray LB, Erikson E, Maller JL. Insulin-stimulated MAP-2 kinase phosphorylates and activates ribosomal protein S6 kinase II. Nature. 1988;334(6184):715–718. [PubMed: 2842685]
37. Dhar A, Young MR, Colburn NH. The role of AP-1, NF-kappaB and ROS/NOS in skin carcinogenesis: the JB6 model is predictive. Mol Cell Biochem. 2002;234–235(1–2):185–193.
38. Zhao J, Bowman L, Zhang X, et al. Titanium dioxide (TiO2) nanoparticles induce JB6 cell apoptosis through activation of the caspase-8/bid and mitochondrial pathways. J Toxicol Environ Health A. 2009;72(19):1141–1149. [PubMed: 20077182]
39. Ding M, Shi X, Dong Z, et al. Freshly fractured crystalline silica induces activator protein-1 activation through ERKs and p38 MAPK. J Biol Chem. 1999;274(43):30611–30616. [PubMed: 10521445]
40. Syrovadko ON, Gracheva KM. Hygienic significance of skin contamination with acetone and the problems of its penetration through the skin. Gig Tr Prof Zabol. 1981;10:23.
41. Ding M, Feng R, Wang SY, et al. Cyanidin-3-glucoside, a natural product derived from blackberry, exhibits chemopreventive and chemotherapeutic activity. J Biol Chem. 2006;281(25):17359–17368. [PubMed: 16618699]
42. Chen Z, Wang Y, Ba T, et al. Genotoxic evaluation of titanium dioxide nanoparticles in vivo and in vitro. Toxicol Lett. 2014;226(3):314–319. [PubMed: 24594277]
43. Rocco L, Santonastaso M, Mottola F, et al. Genotoxicity assessment of TiO2 nanoparticles in the teleost Danio rerio. Ecotoxicol Environ Saf. 2015;113:223–230. [PubMed: 25506637]
44. Nakajima A, Kojima Y, Nakayama M, Yagita H, Okumura K, Nakano H. Downregulation of c-FLIP promotes caspase-dependent JNK activation and reactive oxygen species accumulation in tumor cells. Oncogene. 2008;27(1):76–84. [PubMed: 17599041]
45. Nakano H, Nakajima A, Sakon-Komazawa S, Piao JH, Xue X, Okumura K. Reactive oxygen species mediate crosstalk between NF-kappaB and JNK. Cell Death Differ. 2006;13(5):730–737. [PubMed: 16341124]
46. Lin X, Wang YJ, Li Q, et al. Chronic high-dose morphine treatment promotes SH-SY5Y cell apoptosis via c-Jun N-terminal kinase-mediated activation of mitochondria-dependent pathway. FEBS J. 2009;276(7):2022–2036. [PubMed: 19292871]
47. Jiang XH, Wong BC, Lin MC, et al. Functional p53 is required for triptolide-induced apoptosis and AP-1 and nuclear factor-kappaB activation in gastric cancer cells. Oncogene. 2001;20(55):8009–8018. [PubMed: 11753684]
48. Gu Y, Wang Y, Zhou Q, et al. Inhibition of nickel nanoparticles-induced toxicity by Epigallocatechin-3-Gallate in JB6 cells may be through Down-regulation of the MAPK signaling pathways. PloS One. 2016;11(3):e0150954. [PubMed: 26943640]

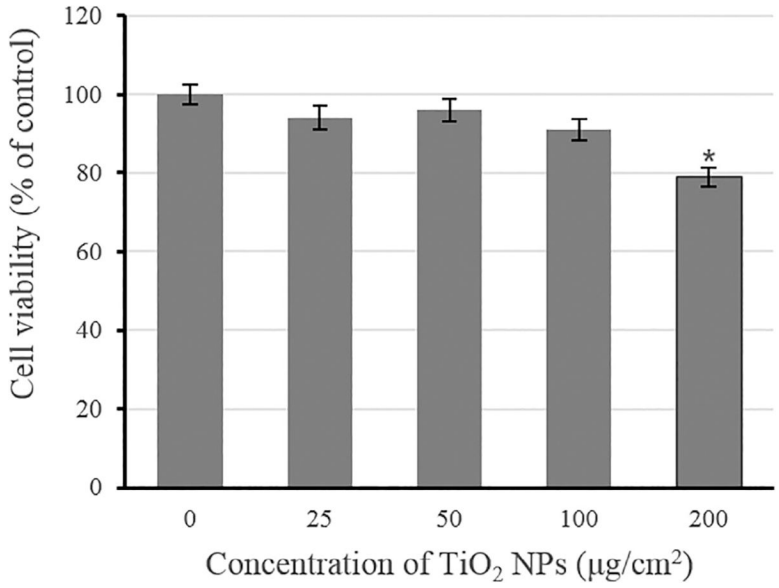

FIGURE 1.

Effects of TiO_2 NPs on cell viability in JB6 cells. Data are expressed as means ± SE ($n = 4$). *$p < .05$, compared with control group

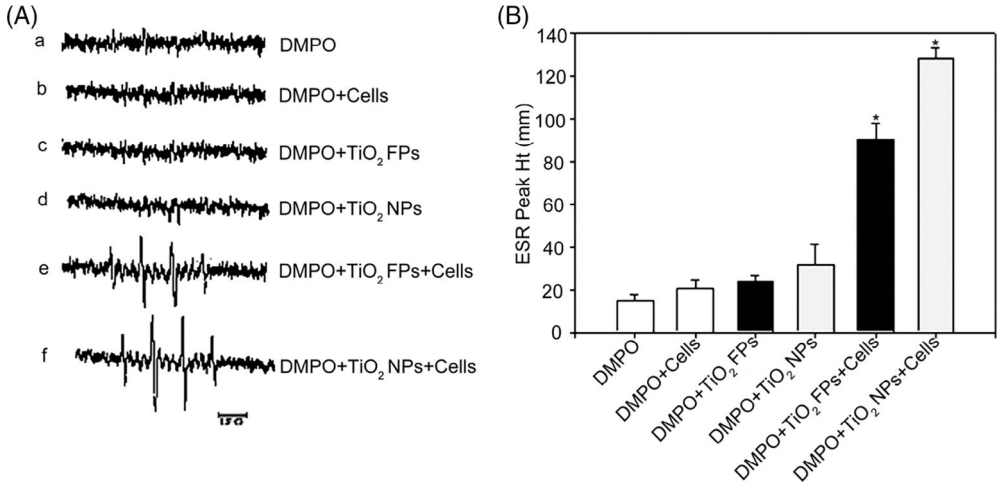

FIGURE 2.

ESR spectra signals (A) and average ESR peak (B) generated by DMPO-OH adducts in different groups. (A) DMPO (200 mM)alone; (B) DMPO (200 mM) + JB6 cells (1×10^6); (C) DMPO (200 mM) + TiO_2 FPs (1 mg/ml); (d) DMPO (200 mM) + TiO_2 NPs (1 mg/ml); (e) DMPO (200 mM) + JB6 cells (1×10^6) + TiO_2 FPs (1 mg/ml); or (F) DMPO (200 mM) + JB6 cells (1×10^6) + TiO_2 NPs (1 mg/ml). The average ESR peak was presented as means ± SE ($n = 3$)

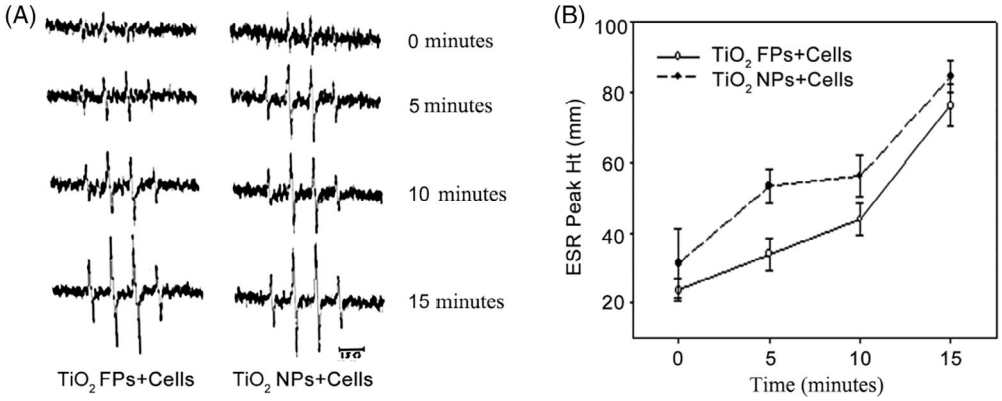

FIGURE 3.

Time-dependent ESR spectra signals (A) and average ESR peak (B) generated by DMPO-OH adducts. The average ESR peak was presented as means ± SE ($n = 3$)

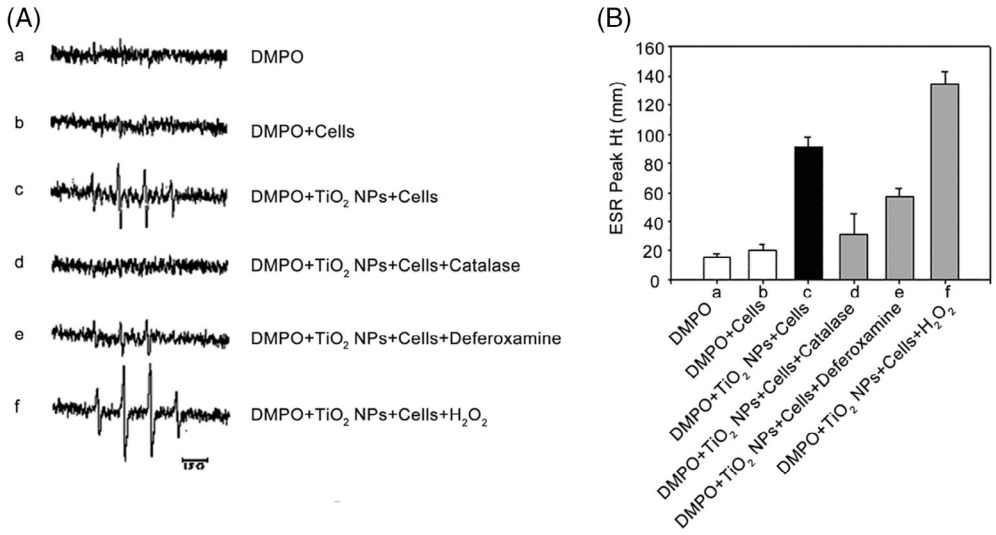

FIGURE 4.

Effects of free radical scavenger on ESR spectra signals (A) and average ESR peak (B) generated by DMPO-OH adducts. (A) DMPO (200 mM); (B) DMPO + JB6 cells (1×10^6); (C) DMPO + TiO_2 NPs (1 mg/ml) + JB6 cells (1×10^6); (D) DMPO + TiO_2 NPs (1 mg/ml) + JB6 cells (1×10^6) + 2000 U/ml catalase; (E) DMPO + TiO_2 NPs (1 mg/ml) + JB6 cells (1×10^6) + deferoxamine (2 mM); (F) DMPO + TiO_2 NPs (1 mg/ml) + JB6 cells (1×10^6) + H_2O_2 (1 mM). (B) The average ESR peak was presented as means ± SE ($n = 3$)

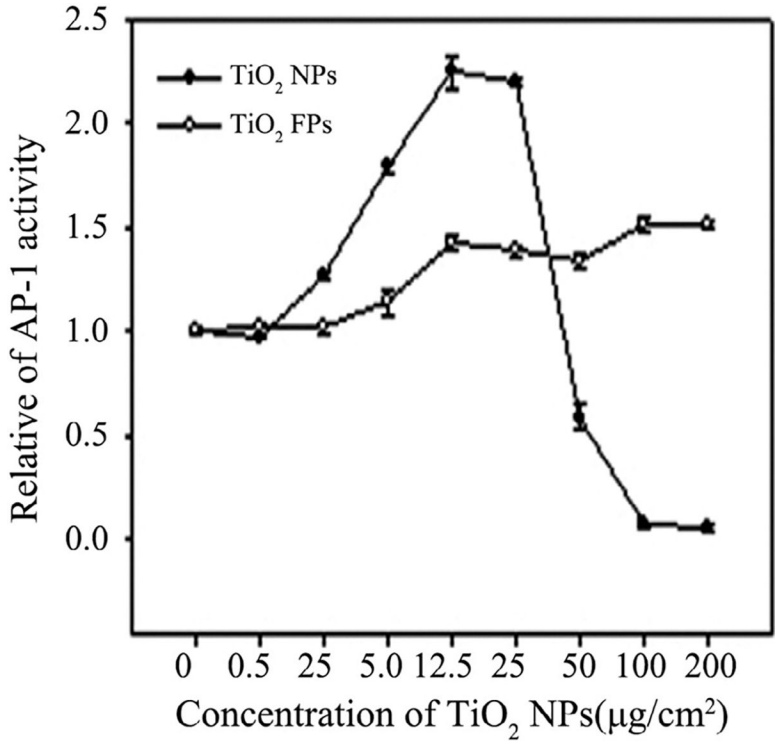

FIGURE 5.

Effect of NPs on induction of AP-1 activation after treatment with JB6 cells for 24 h. Data are presented as the mean ± SE

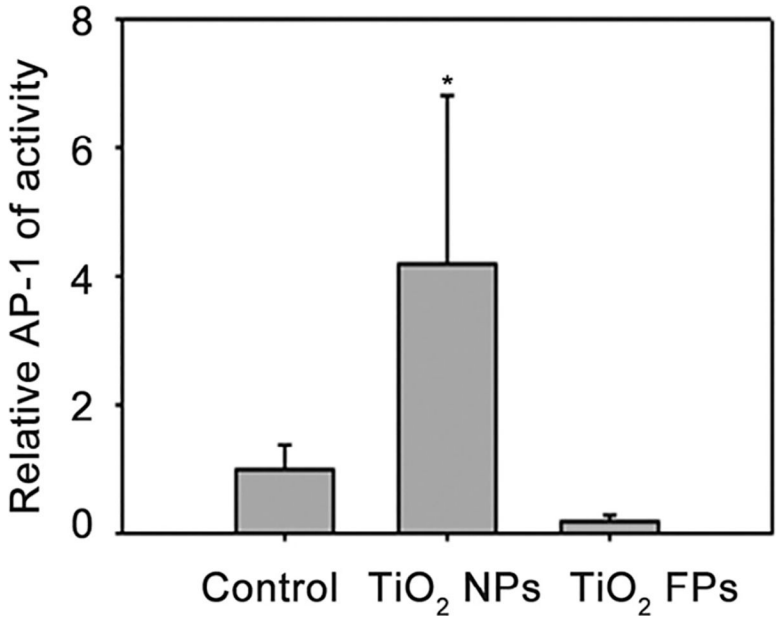

FIGURE 6.

Effect of NPs on the induction of AP-1 activation in the skin tissue of AP-1-luciferase reporter transgenic mice. Relative luciferase units were expressed as means ± SE in 24–28 mice of each group. *$p \leq .05$, compared with control group

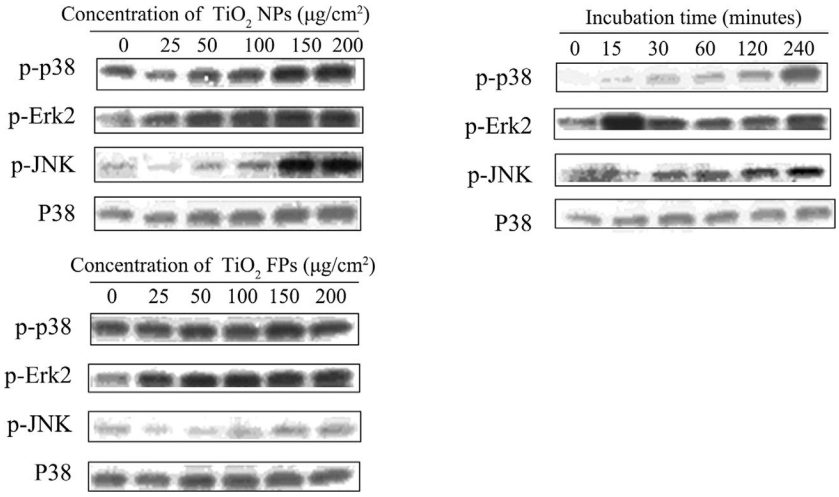

FIGURE 7.

Effect of NPs on the phosphorylation levels of MAPKs determined by Western blotting assay. (A) Stimulation of various concentrations of TiO_2 NPs on the expression levels of p-p38 kinase, p-ERK2, p-JNK and p38; (B) stimulation of various concentrations of TiO_2 FPs on the expression levels of p-p38 kinase, p-ERK2, p-JNK and p38; (C) stimulation of TiO_2 NPs (150 μg/cm^2) on the expression level of p-p38 kinase, p-ERK2, p-JNK and p38 for 15, 30, 60, 120, and 240 min

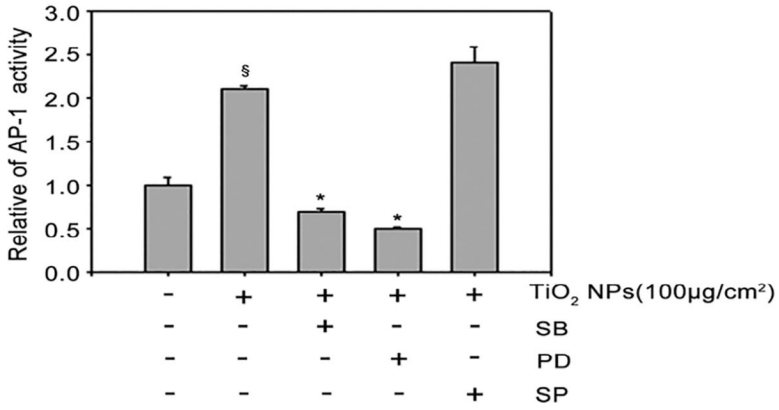

FIGURE 8.

Inhibitory effects of MAPKs inhibitors on TiO_2 NPs-induced AP-1 activation. The relative AP-1 activity was presented as mean ± SE of six test wells from two independent experiments. § $p < .05$, compared with the untreated control group; * $p < .05$, compared with TiO_2 NPs alone group ($p \leq .05$)